

N6-methyladenosine-induced SVIL antisense RNA 1 restrains lung adenocarcinoma cell proliferation by destabilizing E2F1

Zedong Hu, Liang Zhu, Yilin Zhang, and Bing Chen

Second Department of Thoracic Surgery, Anhui Chest Hospital, Hefei, China

ABSTRACT

Accumulating evidence indicates that N6-methyladenosine (m6A) and long noncoding RNAs (lncRNAs) play crucial roles in cancer development. However, the biological roles of m6A and lncRNAs in lung cancer tumorigenesis are largely unknown. In this study, SVIL antisense RNA 1 (SVIL-AS1) was downregulated in lung adenocarcinoma (LUAD) tissues and was associated with a favorable prognosis in patients with LUAD. SVIL-AS1 overexpression suppressed LUAD cell proliferation and blocked cell cycle arrest. Mechanistically, METTL3 increased the m6A modification and transcript stability of SVIL-AS1. The enhanced SVIL-AS1 expression mediated by METTL3 suppressed E2F1 and E2F1-target genes. Moreover, SVIL-AS1 accelerated E2F1 degradation. The reduction in cell proliferation induced by SVIL-AS1 overexpression could be rescued by E2F1 overexpression or METTL3 knockdown. In conclusion, our work demonstrated the role and mechanism of METTL3-induced SVIL-AS1 in LUAD, which connects m6A and lncRNA in lung cancer carcinogenesis.

ARTICLE HISTORY

Received 29 October 2021
Revised 30 December 2021
Accepted 31 December 2021

KEYWORDS

SVIL-AS1; METTL3; E2F1;
lung adenocarcinoma; m6A;
degradation

Introduction

Lung cancer is the leading cause of cancer-related deaths worldwide [1–3]. Adenocarcinoma is the most common subtype of lung cancer, and its prognosis remains poor.




Long noncoding RNAs (lncRNAs) are a type of non-coding transcripts with a minimum length of 200 nucleotides [4–6]. It is reported that lncRNAs can regulate gene expression as enhancers, decoys, guides, and scaffolds [7,8]. Currently, dysregulated lncRNAs are associated with multiple cancer progression, including cell proliferation, cell cycle regulation, epithelial-mesenchymal transition, metastasis, and drug resistance [9–11]. SVIL antisense RNA 1 (SVIL-AS1) was recently found to be downregulated in non-small cell lung cancer (NSCLC) [12]; however, its role and functional significance have not been studied.

N6-methyladenosine (m6A) RNA modification is an important RNA modification involved in the regulation of mRNA stability, splicing, translation, and so on. It plays critical roles in tissue development, self-renewal, and DNA damage response [13–15]. Recent research has revealed that m6A RNA modification plays critical roles in non-coding RNA (ncRNA) metabolism and tumor biological

processes [14,16,17]. It was found that m6A modification of lncRNAs could have an effect on the RNA-protein interaction. For example, lncRNA metastasis-associated lung adenocarcinoma transcript 1 (MALAT1) was reported to be highly associated with tumorigenesis, which was highly m6A methylated [18,19]. In lung cancer, the m6A transferase METTL3-induced lncRNA ABHD11-AS1 was reported to promote the Warburg effect in NSCLC [20]. These findings indicate the vital role of m6A modification in lncRNAs in lung cancer.

The transcription factor E2F1, belonging to the E2 promoter-binding factor (E2F) family, is a key regulator of cell cycle progression, DNA replication, apoptosis, senescence, and metabolism [21–24]. The role and prognostic value of E2F1 has been reported in multiple cancers, including hepatocellular carcinoma [25], colon cancer [26], lung cancer [27], breast cancer [28], and glioma [29]. It is known that E2F1 is involved in cell cycle transition by regulating cell-cycle related genes, growth factors, cytokines [23].

In the present study, we hypothesized that SVIL-AS1 dysregulation could contribute to lung adenocarcinoma (LUAD) development and tumorigenesis.

CONTACT Bing Chen  chenbingSaohu@163.com  Second Department of Thoracic Surgery, Anhui Chest Hospital, Hefei 230022, China
 Supplemental data for this article can be accessed [here](#).

The aim of this study was to investigate the role and potential molecular mechanisms of SVIL-AS1 in LUAD. We identified the prognostic significance of SVIL-AS1 in LUAD among the predicted METTL3-correlated lncRNAs screened from TCGA-LUAD. We validated the consensus m6A modification sites in SVIL-AS1 using MeRIP. METTL3 installed m6A and transcript stability of SVIL-AS1 to enhance its expression. Moreover, SVIL-AS1 overexpression suppressed LUAD cell proliferation and cell cycle arrest at G1 by accelerating E2F1 degradation. Our study reveals that METTL3-induced SVIL-AS1 suppresses the proliferation of LUAD by promoting E2F1 degradation, which advances the understanding of m6A and lncRNA in lung cancer biology.

Materials and methods

Data analysis

Pearson correlation analysis was performed to identify co-expressed lncRNAs related to METTL3 with a cutoff of $|\text{Pearson } R| > 0.3$ and $P < 0.05$, in The Cancer Genome Atlas (TCGA)-LUAD dataset. According to a correlation coefficient greater than 0.3 and a P value less than 0.05, 292 lncRNAs were screened out, from which the top three correlation coefficients were selected for subsequent analysis. Overall survival analysis of lncRNAs from SVIL-AS1 was performed using Kaplan–Meier plotter online tools (<https://kmplot.com/analysis/index.php?p=service&caner=lung>) [30]. Overall survival analysis of lncRNAs from AL731577.2 and NORAD was performed using R software (3.6.3) [31] survminer package (0.4.9). The expression of SVIL-AS1 in LUAD tissues was analyzed using GEPIA2 (<http://gepia2.cancer-pku.cn/#general>) [32] and R software (3.6.3) [31] ggplot2 package (3.3.3).

Expression validation of SVIL-AS1 in GEO datasets

The datasets GSE146461 and GSE85716 downloaded from the GEO database of NCBI (<https://www.ncbi.nlm.nih.gov/geo/>), which were based on GPL20115 (Agilent-067406 Human CBC lncRNA + mRNA microarray V4.0) and GPL19612 (Agilent-062918 OE Human lncRNA Microarray

V4.0 028004), respectively, were used to validate expression of SVIL-AS1. The GSE146461 dataset contained five LUAD samples and three normal tissues. The GSE85716 dataset included six pairs of LUAD tissues and corresponding non-cancerous tissues [33]. The expression of SVIL-AS1 was analyzed in LUAD and normal tissues using the unpaired Student's t-test. Differences in expression values were considered statistically significant if the P-value was < 0.05 .

Cells and cell culture

LUAD cells (A549 and H1650) were purchased from Procell Life Science & Technology Co., Ltd. (Wuhan, China). A549 cells were cultured in Ham's F-12K medium supplemented with 10% fetal bovine serum (FBS) and 100 U/mL penicillin-streptomycin. H1650 cells were maintained in RPMI-1640 medium containing 10% FBS and 1% P/S. The cells were cultured in a humidified atmosphere of 5% CO₂ at 37°C.

Stable cell lines using lentiviral shRNAs

The pLKO-based shRNA clones for METTL3, SVIL-AS1 #1, SVIL-AS1 #2, and the scrambled control were purchased from GenePharma Co., Ltd. (Shanghai, China). All shRNA sequences are described in Table 1. The lentivirus package was used according to the protocols. A549 and H1650 cells were infected with the indicated lentivirus with 10 µg/mL polybrene then selected by 3.3 µg/mL puromycin 48 h after infection. Stable cell lines were maintained in medium containing 3.3 µg/mL puromycin.

Quantitative real-time PCR (qRT-PCR)

RNA was extracted from cells using TRIzol reagent (Invitrogen, USA) and quantified using a NanoDrop spectrophotometer (Thermo Fisher Scientific). RNA was reverse transcribed into cDNA using an EasyScript® One-Step gDNA Removal and cDNA Synthesis SuperMix (Transgene, Beijing, China). qRT-PCR was performed using TransScript® II One-Step RT-PCR SuperMix (Transgene). The relative expression of targets was analyzed using the 7500 real-time PCR system (Applied Biosystems, Foster

Table 1. Sequences for shRNAs.

shRNAs	Oligos
shMETTL3	Sense:5'-ACCTCGCACTTCAGACGAATTATCAATCAAGAGTTGATAATTCGTCTGAAGTGCTT-3' Anti-sense:5'-CAAAAAGCACTTCAGACGAATTATCAACTCTTGATTGATAATTCGTCTGAAGTGCG-3'
shSVIL-AS1#1	Sense:5'-ACCTCGAAAAGCTGCCGGATAAATCATTCAAGAGATGATTATCCGGCAGCTTTCTT-3' Anti-sense:5'-CAAAAAGAAAGCTGCCGGATAAATCATCTTGAATGATTATCCGGCAGCTTTCTG-3'
shSVIL-AS1#2	Sense:5'-ACCTCGGACTTTAGGAACCAACATATCAAGAGTATGTTTGGTTCCTAAAGTCCTT-3' Anti-sense:5'-CAAAAAGGACTTTAGGAACCAACATACTCTTGATATGTTTGGTTCCTAAAGTCCG-3'
Scramble	Sense:5'-ACCTCGCAAATACCAATGCGATGTAATCAAGAGTTACATCGCATTGGTATTGCTT-3' Anti-sense:5'-CAAAAAGCAAATACCAATGCGATGTAACCTTGATTACATCGCATTGGTATTGCG-3'

City, CA, USA) and calculated using the $2^{-\Delta\Delta Ct}$ method [34]. GAPDH was used as an internal control. The primer sequences are shown in Table 2.

Methylated RNA immunoprecipitation PCR (MeRIP-qPCR)

Quantification of m6A-modified SVIL-AS1 was performed by MeRIP-qPCR, as previously described [35]. Total RNA was harvested from A549 or H1650 cells using TRIzol reagent. Two micrograms of anti-m6A antibody (ab151230, Abcam, Burlingame, CA, USA) or anti-IgG (Cell Signaling Technology) were conjugated to the protein A/G magnetic beads at 4°C for 4 h in IP buffer (20 mM Tris pH 7.5, 140 mM NaCl, 1% NP-40, 2 mM EDTA). Then, the fragmented RNA was incubated with the antibody in IP buffer supplemen-

ted with RNase inhibitor and protease inhibitor on a rotator at 4°C overnight. Then, the RNA was eluted using evolution buffer (50 mM Tris-HCl pH 7.5, 150 mM NaCl, 1 mM EDTA, 0.1% SDS, 20 mM DTT). The immunoprecipitated RNA was used for qRT-PCR assays. SVIL-AS1 primer for MeRIP-qPCR F1 F: 5'-TCTACCTCATGCTCTTATG-3'; R: 5'-TGCTTATGTTTGGTTCCTAA-3'. SVIL-AS1 primer for MeRIP-qPCR F2 F: 5'-CTATAAAGAGCGAGAGTAGA-3'; R: 5'-TGAATATTCACACAAAAGGAAC-3'.

RNA stability analysis

LUAD cells were treated with actinomycin D (Act-D, 5 µg/mL) at different times. RNA was extracted using TRIzol at the indicated times and

Table 2. Primers for qRT-PCR.

Genes	Sequences
METTL3	Forward 5'-TTGTCTCCAACCTTCCGTAGT-3' Reverse 5'-CCAGATCAGAGAGGTGGTGTAG-3'
E2F1	Forward 5'-ACGCTATGAGACCTCACTGAA-3' Reverse 5'-TCCTGGGTCAACCCCTCAAG-3'
CCNE1	Forward 5'-GCCAGCCTGGGACAATAATG-3' Reverse 5'-CTTGACGTTGAGTTTGGGT-3'
MYBL2	Forward 5'-CTTGAGCGAGTCCAAAGACTG-3' Reverse 5'-AGTTGGTCAGAAGACTTCCCT-3'
CDC25A	Forward 5'-CTCCTCCGAGTCAACAGATTCA-3' Reverse 5'-CAACAGCTTCTGAGGTAGGGA-3'
p27	Forward 5'-ATCACAAACCCTAGAGGGCA-3' Reverse 5'-GGGTCTGTAGTAGAACTCGGG-3'
p15	Forward 5'-GGGACTAGTGGAGAAGGTGC-3' Reverse 5'-CATCATCATGACCTGGATCGC-3'
SVIL-AS1	Forward 5'-ACAGAAATCCTAACGGGGCG-3' Reverse 5'-CCATGATCTGATCCCTGCC-3'
GAPDH	Forward 5'-CTGGGCTACACTGAGCACC-3' Reverse 5'-AAGTGGTCTGTTGAGGGCAATG-3'

E2F1 promoter (F-5'TTCGCGCAAAAAGGATTT; R- 5'GCCGCTGCTGCAAAGT),GGGACTAGTGGAGAAGGTGC CATCATCATGACCTGGATCGC

the relative expression of mRNA was detected by qRT-PCR [36].

Cell counting Kit 8 (CCK-8)

Cell viability was analyzed using the Cell Counting Kit 8 (CCK-8, Beyotime, Beijing, China). The transfected cells were seeded in a 96-well plate at a density of 10^4 /well. Cells were cultured for 24, 48, 72, or 96 h. Then, the cells in each well were incubated with 10 μ L CCK-8 reagent for 2 h. The absorbance at 450 nm (optical density, 450 nm) was detected using a microplate reader (Thermo Fisher Scientific).

Protein stability analysis

Cells were treated with cycloheximide (CHX, final concentration 100 μ g/mL), vehicle (DMSO), MG132 (20 nM), or 3-MA (25 nM) for the indicated times. Western blotting was performed to analyze protein levels.

BrdU labeling

BrdU labeling was detected using 5-Bromo-2-deoxy-Uridine (BrdU; Roche, Basel, Switzerland). The cells were seeded into 24-well plates at a density of 0.2×10^5 /well. The cells were transfected as described previously. After 48 h, the cells were incubated with 10 μ M BrdU for 2 h at 37°C. The cells were fixed with 4% paraformaldehyde and permeabilized with 0.2% Triton X-100. After incubation in 1.5 M HCL, cells were washed with PBS. Then, the cells were incubated with BrdU antibody (1:1000) and incubated at 4°C overnight. The cells were stained with DAPI for nuclear staining. Images were captured using a fluorescence microscope.

Cell cycle analysis

The cells were harvested and fixed with 70% ethanol at 4°C overnight. The cells were incubated with propidium iodide (PI, 1 μ g/mL) solution containing RNase A (10 mg/mL, Sigma-Aldrich, St. Louis, MA, USA) for 1 h and wrapped in foil at 4°C. Cell cycle analysis was performed using a FACScan Flow Cytometer (Becton-Dickinson) and analyzed using FlowJo LLC software (Ashland, OR).

Nuclear-cytoplasmic fractionation

Total RNA was isolated from cells using the TRIzol reagent (Invitrogen). RNA from the nucleus and cytoplasm of LUAD cells was separated using the PARIS™ Kit (Invitrogen, USA). U6 RNA was used as a nuclear control, and GAPDH mRNA was used as a cytoplasmic control. The fractionated RNA was detected by qRT-PCR.

Western blot

Total protein was extracted from cancer cells and the protein concentration was determined using a bicinchoninic acid protein assay kit (Beyotime). The protein was separated using 10% SDS-PAGE and transferred onto a polyvinylidene fluoride membrane (EMD Millipore, Bedford, USA). The membranes were blocked with 5% nonfat milk for 1 h at room temperature, and then incubated with specific primary antibodies against E2F1 (1:500, Bioss, Beijing, China), METTL3 (1:1000, Abcam), and GAPDH (1:1000, Bioss) overnight at 4°C. Next, the membranes were incubated with the appropriate secondary antibodies for 1 h at room temperature. The bands were detected using enhanced chemiluminescence.

Xenograft tumor models

All mouse experiments were carried out by Beijing Viewsolid Biotech Co., Ltd., and the animal ethics approval form was 201901003. Male BALB/c mice (6 weeks old, ~18 g) were purchased from Sib Biotechnology Co., Ltd. (Beijing, P.R. China). A549 cells (1×10^6 cells) were intraperitoneally injected into the abdomen of nude mice. Tumor length and width were measured and recorded every 4 days after inoculation. Tumor volume was calculated as $1/2 \times \text{length} \times \text{width}^2$. The tumor weight was weighed and recorded 20 days after inoculation.

Statistical analysis

Data were analyzed using the GraphPad Prism version 8. Data are presented as mean \pm SD. The two-tailed Student's *t*-test was used to compare gene expression between the two groups. One-way analysis of variance (ANOVA) was used to analyze the differences among multiple groups.

Pearson's correlation analysis was used to analyze the correlation between METTL3 and lncRNAs in LUAD samples. The Kaplan–Meier method was used to analyze the overall survival of LUAD patients with higher or lower lncRNA expression. Statistical significance was set at $P < 0.05$.

Results

Based on the finding that SVIL-AS1 was down-regulated in LUAD tissues and had a prognostic value for LUAD, we speculated that SVIL-AS1 might act as a tumor suppressor in LUAD tumorigenesis. The goal of this study was to verify the role and regulatory mechanisms of SVIL-AS1 in LUAD. Functionally, CCK-8, BrdU staining, and cell cycle analysis were performed to analyze the effect of SVIL-AS1 on cell proliferation and cell cycle. Mechanistically, METTL3 was found to be upstream of SVIL-AS1 via m6A modification. Rescue experiments were performed to confirm that E2F1 is a downstream target of SVIL-AS1.

Down-regulated SVIL-AS1 is associated with an unfavorable prognosis in LUAD

We screened the METTL3-correlated lncRNAs in the TCGA-LUAD database using Pearson's correlation analysis which was restricted to $|\text{Pearson } R| > 0.3$ and $P < 0.05$, and obtained the top three lncRNAs (SVIL-AS1, AL731577.2, NORAD) according to the correlation coefficient in descending order. ($R_{\text{SVIL-AS1}} = 0.657$, $R_{\text{AL731577.2}} = 0.590$, $R_{\text{NORAD}} = 0.571$, $P < 0.001$. [Figure 1\(a\)](#)). For further research, we analyzed their prognostic values using the Kaplan–Meier plotter and found that only SVIL-AS1 had prognostic significance in LUAD ([Figure 1\(b\)](#)). That is, high expression of SVIL-AS1 was associated with prolonged survival time in patients with LUAD. SVIL-AS1 was down-regulated in LUAD tumor tissues compared to normal tissues by GEPIA2, of which the samples were from the TCGA and GTEx projects. ([Figure 1\(c\)](#)). In addition, the level of SVIL-AS1 was also lower in paired and unpaired LUAD tumor tissues than in normal tissues from the TCGA-LUAD database ([Figure 1\(d\)](#)). The relationship between SVIL-AS1 and LUAD was also validated in the GEO database. SVIL-AS1 was downregulated in

GSE85716 and GSE146461 [[33](#)] ([Figure 1\(e\)](#)). Above all, these data suggest that SVIL-AS1 has a favorable prognostic value in LUAD and might play a tumor-suppressive role in LUAD.

METTL3-mediated m6A modification is critical for SVIL-AS1 stability

To investigate whether RNA methyltransferase-like 3 (METTL3) plays a role in the regulation of SVIL-AS1, we analyzed the potential m6A modification sites by METTL3 on the SVIL-AS1 sequence via the SRAMP (cuilab.cn/sramp/) [[37](#)]. Three m6A sites with very high confidence were identified in the SVIL-AS1 sequence before the 3'-untranslated regions (3'-UTR). We designed two pairs of PCR primers to identify nearby m6A methylation motifs ([Figure 2\(a\)](#)). To verify the presence of m6A methylated positions, we performed RNA immunoprecipitation using the m6A antibody in A549 and H1650 cells. As shown in [Figure 2\(b\)](#), there were m6A methylation sites in the SVIL-AS1 sequence by PCR1 and PCR2. To further confirm the m6A sites by METTL3, we performed m6A immunoprecipitation in METTL3-silence cells. As expected, the PCR1 and PCR2 fragments (containing the m6A modification sites) decreased significantly when METTL3 was silenced ([Figure 2\(c,d\)](#)), which validates the presence of m6A sites mediated by METTL3. Furthermore, RNA stability analysis showed that METTL3 knockdown reduced the stability of SVIL-AS1 ([Figure 2\(e\)](#)). Taken together, these data indicate that METTL3 is critical for SVIL-AS1 stability in an m6A modification manner.

SVIL-AS1 inhibits LUAD cells proliferation and contributes to cell cycle arrest

To explore the biological function of SVIL-AS1 in LUAD cells, we knocked down or overexpressed SVIL-AS1 in A549 and H1650 cells using short hairpin RNA (shRNA) or the pcDNA3.1 vector. Overexpression of SVIL-AS1 was measured by RT-qPCR, as shown in [Figure 3\(a\)](#). CCK-8 analysis showed that SVIL-AS1 overexpression inhibited the proliferation of A549 and H1650 cells ([Figure 3\(b\)](#)). Forced expression of SVIL-AS1

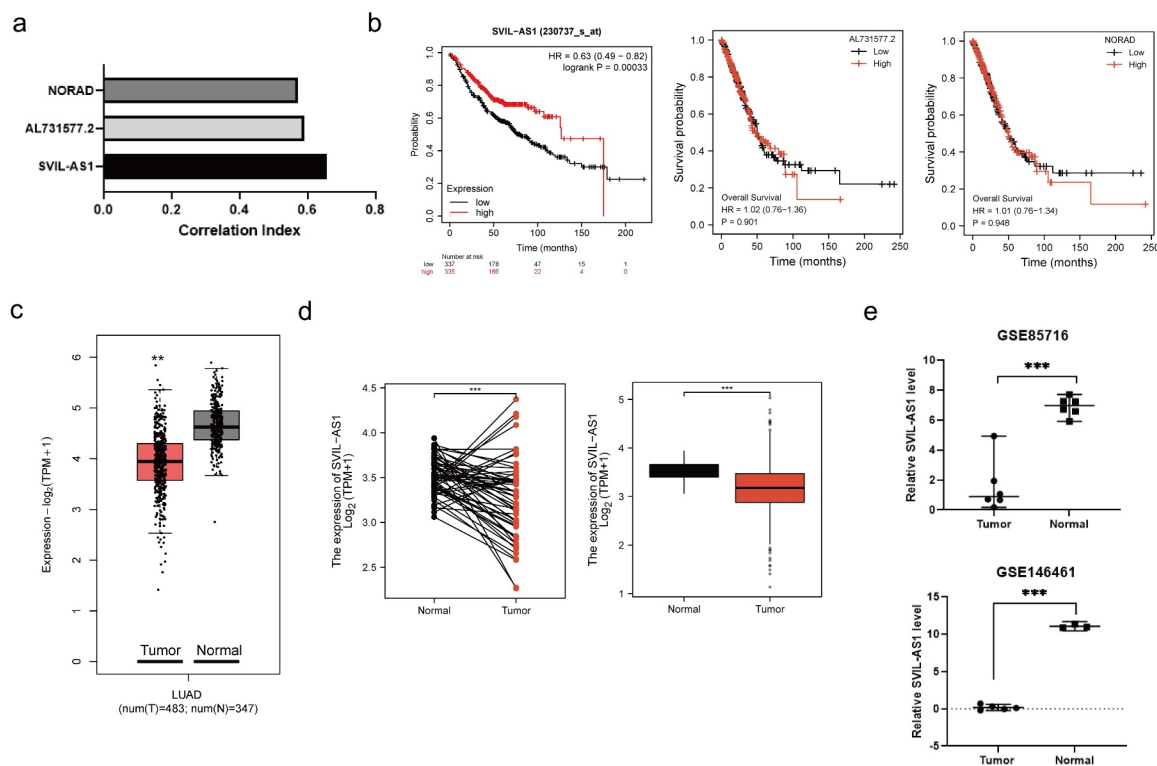


Figure 1. SVIL-AS1 is down-regulated and has a prognostic value in LUAD. (a) Schematic image of the screened top three METTL3-correlated lncRNAs with a cutoff of $|\text{Pearson } R| > 0.3$ and $P < 0.05$, in TCGA-LUAD dataset. $R_{\text{SVIL-AS1}} = 0.657$, $R_{\text{AL731577.2}} = 0.590$, $R_{\text{NORAD}} = 0.571$. $P < 0.001$. (b) The overall survival analysis of LUAD patients with SVIL-AS1, AL731577.2, and NORAD expression was analyzed using the Kaplan–Meier plotter. (c) The relative expression of SVIL-AS1 was analyzed in LUAD normal and tumor tissues using GEPIA2. The red box indicates tumor tissues, and the black box indicates normal tissues. $** P < 0.01$. (d) The level of SVIL-AS1 was analyzed in paired LUAD tumor samples ($n = 57$, left). SVIL-AS1 expression was analyzed in unpaired LUAD tumor tissues ($n = 535$) and normal tissues ($n = 59$, right). $*** P < 0.001$. (e) SVIL-AS1 levels were validated using GSE85716 and GSE146461. $*** P < 0.001$.

also reduced BrdU-positive cells (Figure 3(c)) and arrested the cell cycle at the G1 phase (Figure 3(d)). These data demonstrate that SVIL-AS1 inhibits cell proliferation and blocks the cell cycle in LUAD cells.

METTL3-mediated SVIL-AS1 down-regulates E2F1 and E2F1-target genes in LUAD cells

Considering that E2F1 is known as a key regulator of the G1/S phase transition [23], based on the above result of SVIL-AS1 silencing induced G1 phase arrest in LUAD cells, we evaluated the expression of cell cycle transition related genes, including E2F1 and E2F1-target genes such as cyclin E1 (CCNE1), Myb-like protein 2 (MYBL2), phospho-Ser/Tr phosphatase cdc25A (CDC25A) [38,39] and cell cycle regulators such as p27 and p15 [40–42] in LUAD cells,

respectively. As shown in Figure 4(a,b), we observed that there was a significant increase in E2F1, CCNE1, MYBL2, and CDC25A in SVIL-AS1-knockdown cells, but no obvious alteration in the relative expression of p27 and p15, suggesting that SVIL-AS1 might affect cell proliferation and cell cycle by regulating E2F1 and E2F1-target genes (CCNE1, MYBL2, and CDC25A). Additionally, we examined whether SVIL-AS1 influenced E2F1 promoter activity. The E2F-luciferase activity was not obviously changed in SVIL-AS1-overexpression cells compared to the control, as shown in Figure S1. To assess whether METTL3-induced SVIL-AS1 in the regulation of E2F1 and its target genes expression, we performed qPCR in SVIL-AS1-forced-expressed cells by silencing METTL3. The results showed that the downregulation of E2F1, CCNE1, MYBL2, and CDC25A could be rescued by METTL3 knockdown (Figure 4(c,d)). These

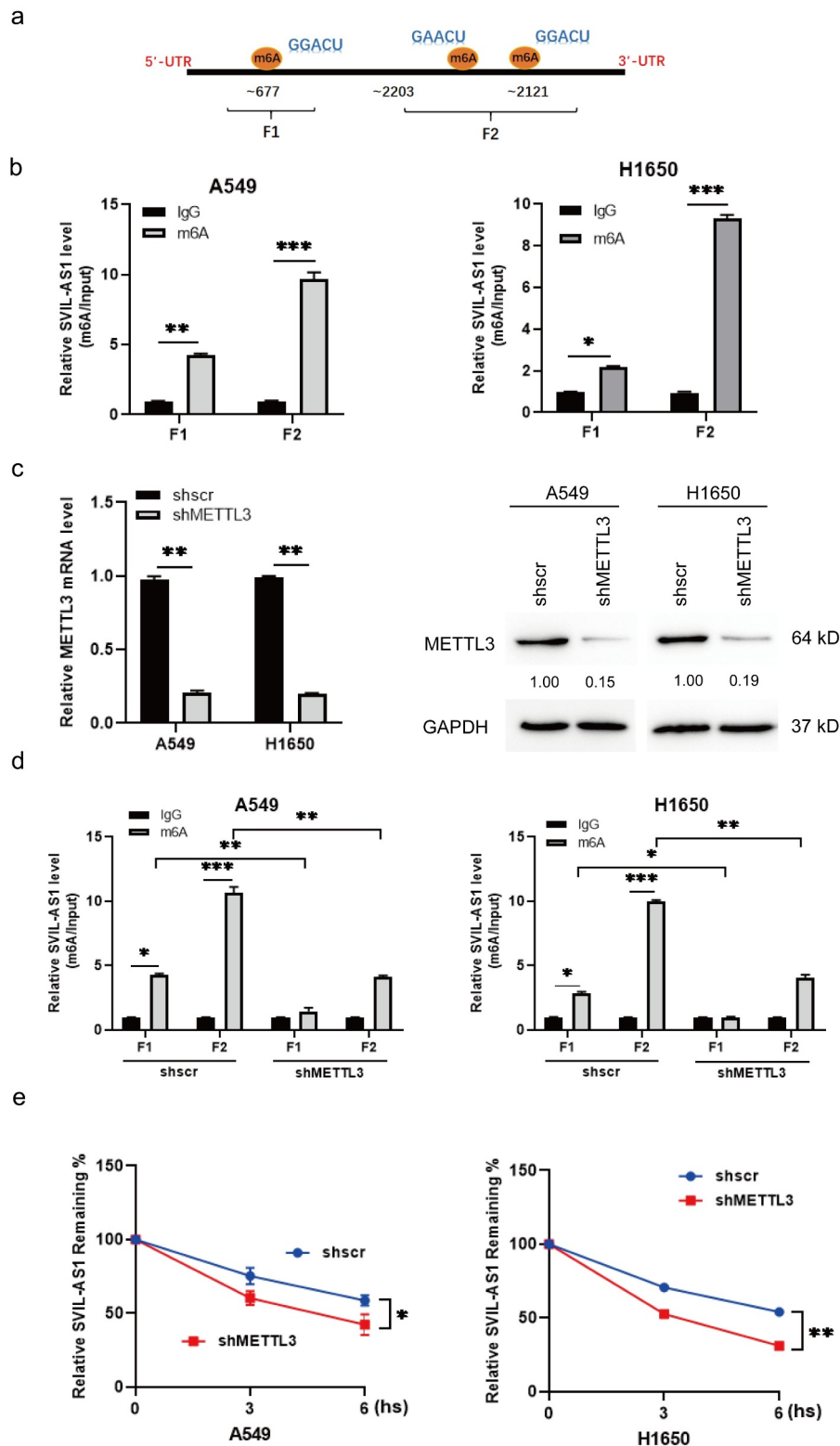


Figure 2. METTL3 silence contributes to the reduced m6A modification and stability of SVIL-AS1. (a) Schematic diagram of the predicted m6A modification sites by METTL3 on the SVIL-AS1 sequence. Two pairs of primers for different SVIL-AS1 fragments containing the m6A sites are indicated as fragment 1 (F1) and fragment 2 (F2). (b) M6A immunoprecipitation was performed in A549 and H1650 cells using an m6A antibody. The relative expression levels of F1 and F2 were measured using qRT-PCR. * $p < 0.05$, ** $p < 0.01$. (c) The knockdown efficiency of shMETTL3 was determined in A549 and H1650 cells by qPCR and Western blotting. (d) M6A immunoprecipitation was performed in A549 and H1650 cells with METTL3 knockdown. The relative expression levels of F1 and F2 were measured using qRT-PCR. * $p < 0.05$, ** $p < 0.01$. (e) The stability of SVIL-AS1 was analyzed in METTL3-silenced A549 and H1650 cells with actinomycin D (Act-D, 5 $\mu\text{g}/\text{mL}$) treatment. * $p < 0.05$, ** $p < 0.01$.

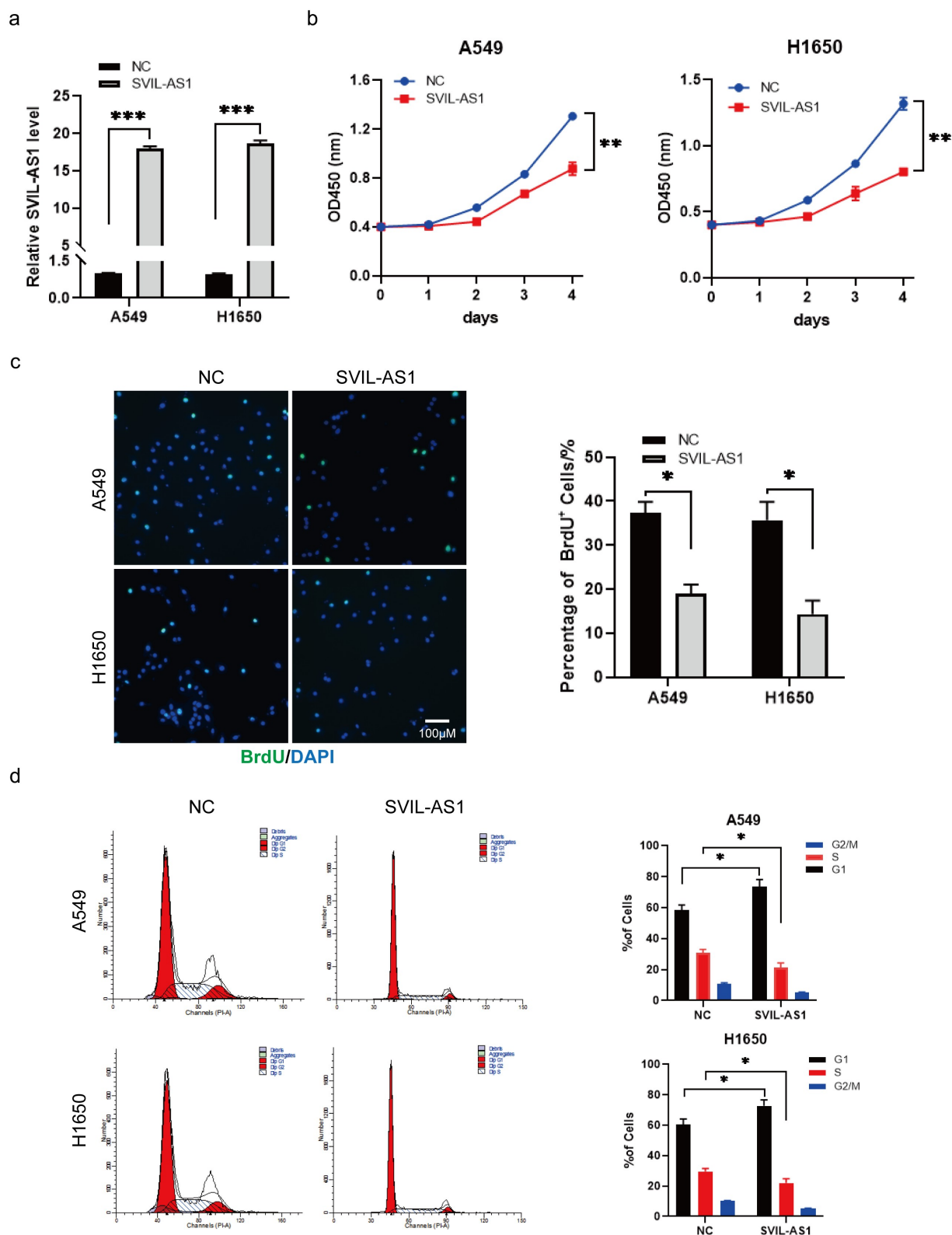


Figure 3. SVIL-AS1 overexpression leads to the decreased cell proliferation and cell cycle arrest of LUAD. (a) The relative expression of SVIL-AS1 was determined in SVIL-AS1-knockdown and forced-expressing cells by qRT-PCR in A549 and H1650 cells. (b–d) CCK-8 assay (b), BrdU staining (c), and cell cycle analysis (d) were performed in A549 and H1650 cells overexpressing SVIL-AS1. * $p < 0.05$, ** $p < 0.01$, *** $p < 0.001$.

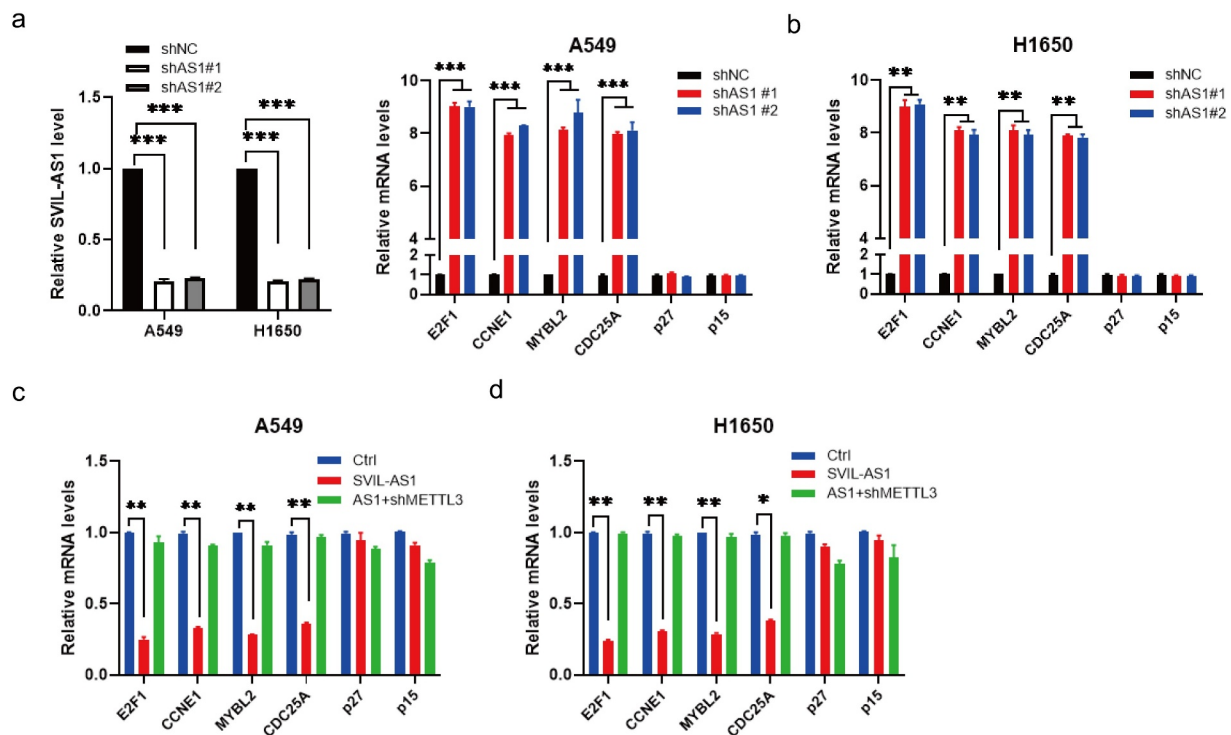


Figure 4. METTL3-mediated SVIL-AS1 suppresses E2F1 and E2F1-target genes in LUAD cells. (a,b) A549 and H1650 cells were transfected with shSVIL-AS1 #1, shSVIL-AS1 #2 or shscr. The relative expression of E2F1, CCNE1, MYBL2, CDC25A, p27 and p15 was determined by qRT-PCR. (c,d) A549 and H1650 cells were cotransfected with shMETTL3 and/or SVIL-AS1. The relative expression of E2F1, CCNE1, MYBL2, CDC25A, p27 and p15 was determined by qRT-PCR. * $p < 0.05$, ** $p < 0.01$, *** $p < 0.001$.

results indicate that SVIL-AS1 suppresses the expression of E2F1 and its target genes in LUAD cells, of which the regulation METTL3 participated in.

SVIL-AS1 accelerates E2F1 degradation

Increasing number of studies have revealed that lncRNAs may function as scaffolds to regulate gene expression [43,44]. First, we predicted the cellular localization of SVIL-AS1 using the online tools lncATLAS, lncLocator, and RNALOCATE, and the results showed that lncRNA SVIL-AS1 was distributed in the nucleus and cytoplasm (Figure 5(a)). We verified the location of SVIL-AS1 by separating the cytoplasm and nucleus of A549 and H1650 cells (Figure 5(b)). We observed that silencing of SVIL-AS1 increased the protein level of E2F1 in both A549 and H1650 cells, while forced expression of SVIL-AS1 decreased E2F1 protein expression in LUAD cells (Figure 5(c,d)). We treated cells with CHX, a protein synthesis inhibitor. The downregulation of E2F1 protein was observed to be much faster in SVIL-AS1-overexpressed cells than in control cells (Figure 5(e)).

In contrast, SVIL-AS1 silencing reduced the downregulation of E2F1 following CHX treatment (Figure 5(f)). These findings suggest that SVIL-AS1 may regulate E2F1 protein degradation, such as the ubiquitin/proteasomal pathway or autophagy/lysosomal pathway. To identify the specific degradation pathway, we treated cells with the proteasome inhibitor MG132 and lysosome inhibitor 3-MA, respectively. MG132 treatment abolished the SVIL-AS1-overexpression-induced downregulation of E2F1 protein, but not 3-MA (Figure 5(g)). Consistently, the increased E2F1 protein level in SVIL-AS1-silenced cells was much higher with MG132 treatment, but not with 3-MA treatment, than in the control cells (Figure 5(h)). These data demonstrate that SVIL-AS1 regulates E2F1 protein degradation via ubiquitination.

SVIL-AS1 regulated by METTL3 restrains LUAD cell proliferation via E2F1

To investigate the regulatory mechanism of SVIL-AS1 in LUAD cell proliferation and the cell cycle, we performed rescue assays. CCK-8, BrdU staining,

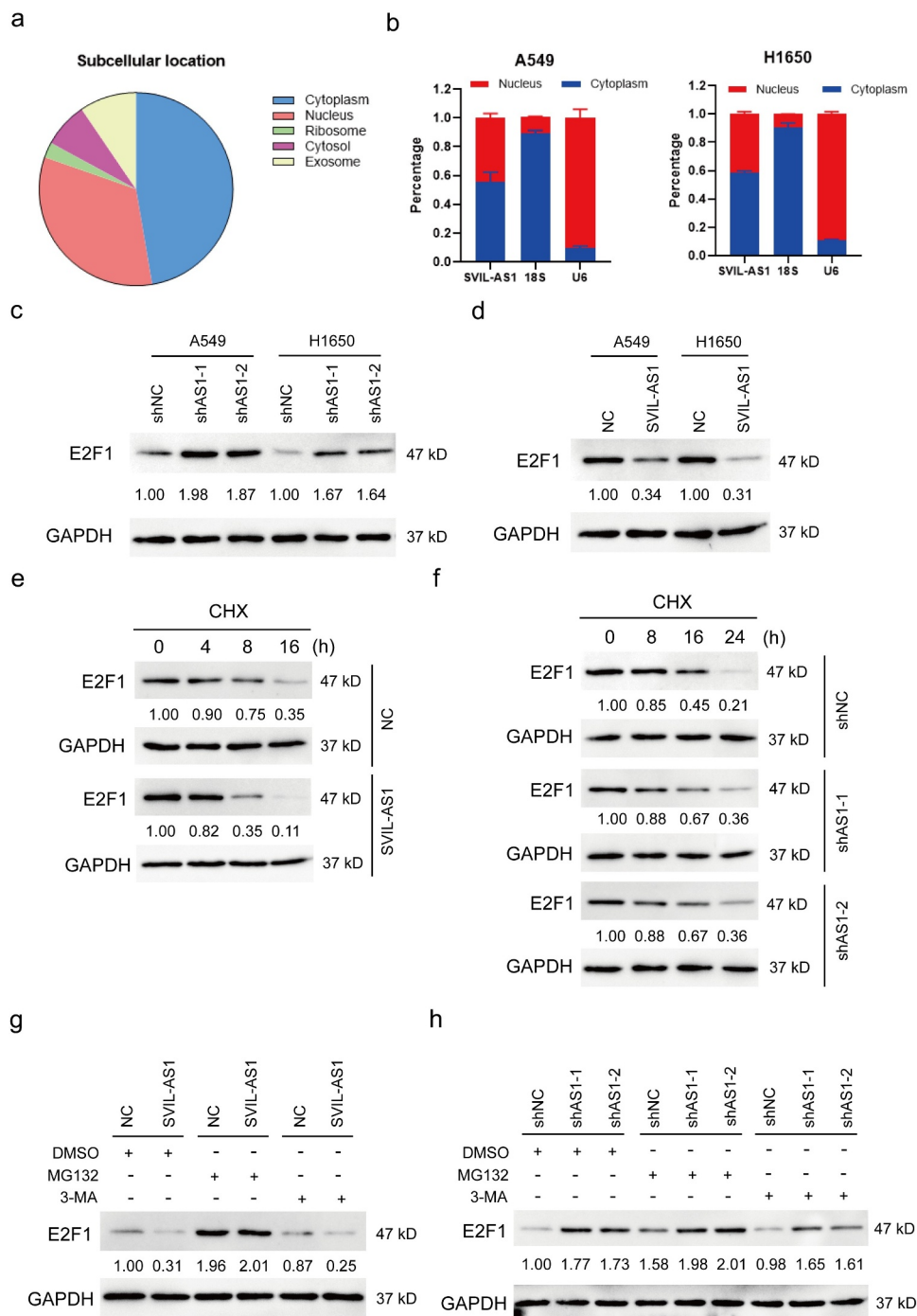


Figure 5. SVIL-AS1 accelerates E2F1 degradation. (a) The cell location of SVIL-AS1 was predicted using the online tools IncAtlas, IncLocator, and RNALOCATE. (b) The subcellular distribution of SVIL-AS1 was detected in A549 and H1650 cells. (c,d) The protein level of E2F1 was measured in A549 and H1650 cells with SVIL-AS1 overexpression or knockdown. (e,f) E2F1 protein levels were detected in A549 and H1650 cells with SVIL-AS1 overexpression or knockdown with cycloheximide (CHX) treatment for 0, 8, 16, 24 h. (g,h) E2F1 protein levels were detected in A549 and H1650 cells with SVIL-AS1 overexpression or knockdown with MG132 (20 nM) treatment or DMSO (control) or 3-MA (50 nM).

and cell cycle analysis indicated that SVIL-AS1 overexpression inhibited cell proliferation, reduced BrdU-positive cells, and cell cycle arrest at the G1 phase (Figure 6(a-c)). However, co-transfection

(E2F1 overexpression plus SVIL-AS1 overexpression, and METTL3 knockdown plus SVIL-AS1 overexpression) restored the inhibitory effects on cell proliferation and cell cycle arrest. Moreover,

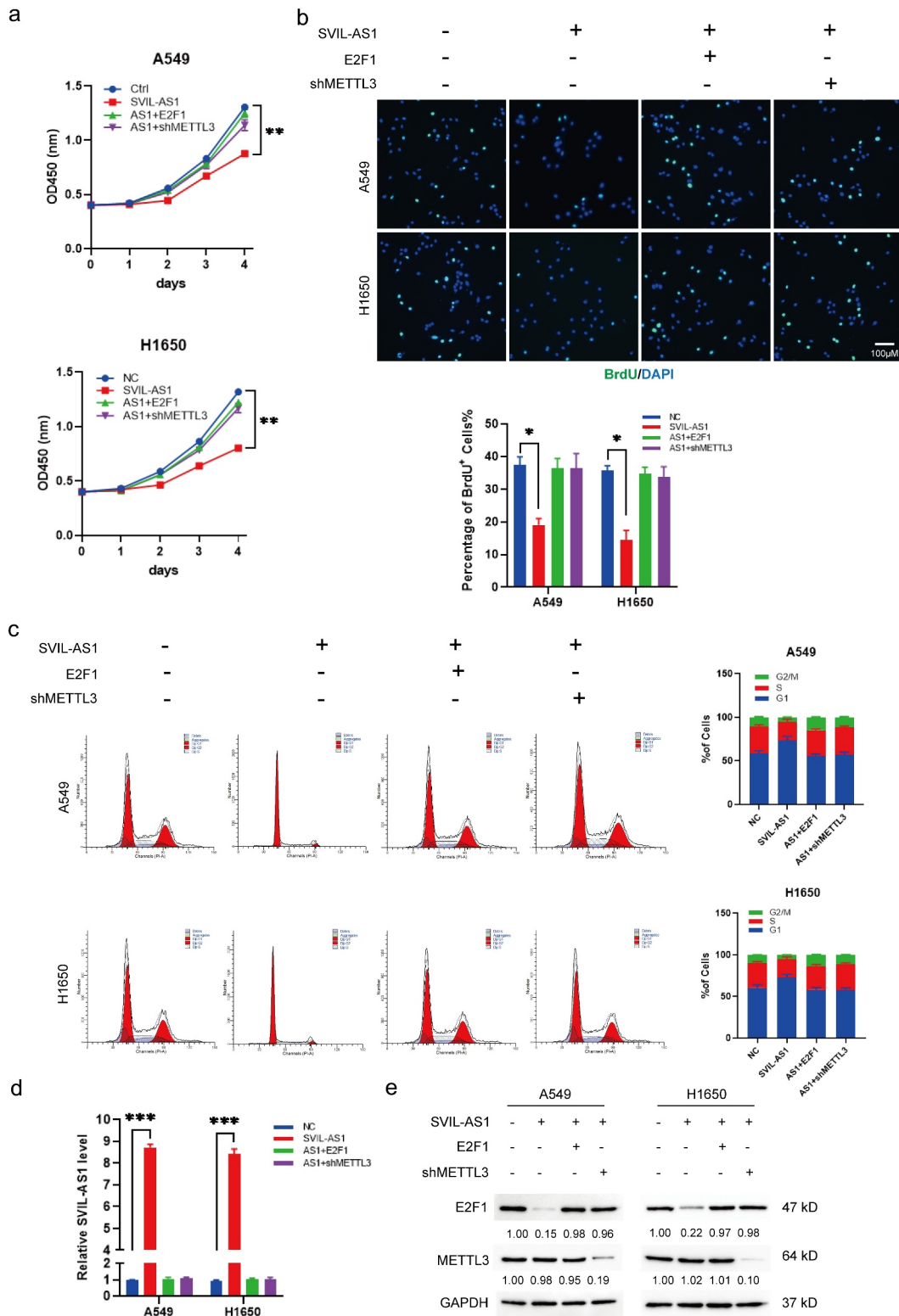


Figure 6. METTL3 regulated SVIL-AS1 has an inhibitory effects on cell proliferation of LUAD by E2F1. (a) CCK-8 assay (b) BrdU staining and (c) cell cycle analysis were performed to detect cell viability, cell proliferation, and cell cycle transition. A549 and H1650 cells were co-transfected with SVIL-AS1 overexpression, E2F1 overexpression, or shMETTL3 overexpression. * $p < 0.05$, ** $p < 0.01$, *** $p < 0.001$. (d,e) The relative expression of E2F1 and METTL3 was detected by qPCR and Western blotting in A549 and H1650 cells co-transfected with SVIL-AS1 overexpression plus E2F1 overexpression or shMETTL3. The relative expression of SVIL-AS1 was measured by qPCR. * $p < 0.05$, ** $p < 0.01$, *** $p < 0.001$.

the decreased E2F1 protein level induced by forced SVIL-AS1 expression could be rescued by METTL3 knockdown or E2F1 overexpression in SVIL-AS1-overexpressed cells (Figure 6(d,e)). In summary, our data suggest that METTL3-SVIL-AS1, stabilized by METTL3 via m6A modification, suppressed LUAD cell proliferation and blocked cell cycle transition by promoting E2F1 degradation.

SVIL-AS1 suppressed tumor growth in vivo

To validate the role and regulatory mechanism of SVIL-AS1 in LUAD, we performed *in vivo* experiments. We established a xenograft tumor model for LUAD. We observed that the tumor volume and weight decreased significantly in the SVIL-AS1-group compared to the NC group. However, E2F1 overexpression or METTL3 knockdown rescued the inhibitory effects of SVIL-AS1 overexpression (Figure 7(a-c)). These findings were consistent with the *in vitro* results, indicating that SVIL-AS1 could act as a tumor suppressor in LUAD tumorigenesis via the METTL3/SVIL-AS1/E2F1 axis.

Discussion

M6A modification (in both coding and non-coding RNAs) has been reported to play critical roles in almost all biological processes, including tumor development and drug resistance. In this study, it was the first time to identify the anti-tumor role of SVIL-AS1 in lung adenocarcinoma, which was associated with a favorable prognosis of patients with LUAD. SVIL-AS1 is located on chromosome 10q13, and very little research has addressed its role or regulatory function. We observed that SVIL-AS1 overexpression could inhibit lung adenocarcinoma cell proliferation and induced cell cycle arrest at G1. Additionally, we found that METTL3 installed the SVIL-AS1 m6A modification and maintained its stability. Elevated SVIL-AS1 expression decreased the cell cycle regulator E2F1 and its target genes CCNE1, MYBL2, and CDC25A. Thus, our data highlight the effect of lncRNA -m6A regulatory network on lung cancer and first elucidate the role of m6A methylation modified lncRNA SVIL-AS1 in the regulation of E2F1 in lung adenocarcinoma.

It is well known that dysregulation of lncRNAs is associated with tumor initiation, development,

and progression [45,46]. LncRNAs can control gene expression at the transcriptional, post-transcriptional, and translational levels, and thus influence various biological processes such as proliferation, metastasis, survival, inflammation, and metabolism [47,48]. Increasing evidence has elaborated the underlying mechanisms of lncRNAs at diverse regulatory levels; for instance, lncRNAs can function as miRNA sponges at the transcriptional level. LncRNA BCRT1 competitively binds with miR-1303 to prevent the degradation of its target gene PTBP3, which acts as a tumor promoter in breast cancer 32384893. LncRNAs can also act as scaffolds by participating in post-translational modifications such as ubiquitination and phosphorylation. For example, lncRNA LINRIS blocked K139 ubiquitination of IGF2BP2 and prevented its degradation in colorectal cancer [49]. In this study, SVIL-AS1 was predicted in the cytoplasm and nucleus, suggesting that it might function as a competing endogenous RNA, microRNA sponge, or transcriptional regulator. Interestingly, we observed that SVIL-AS1 did not regulate E2F1 at the transcriptional level because there was no alteration in its transcription factor activity. However, SVIL-AS1 knockdown blocked E2F1 degradation caused by MG132 treatment, suggesting that SVIL-AS1 accelerated E2F1 degradation in the ubiquitin-proteasome pathway at the post-transcriptional level.

E2F1 has been shown to play critical roles in multiple cancers, including lung cancer [50–52]. For instance, E2F1 and EIF4A3 facilitated the carcinogenesis and development of triple-negative breast cancer through the circSEPT9/miR-637/LIF axis [28]. E2F1 is deubiquitylated and stabilized by POH1 to promote liver tumor formation 26,510,456. In NSCLC, SRPK2 downregulation promotes cell cycle arrest though E2F1 [53]. In this study, we observed that forced SVIL-AS1 expression inhibited cell proliferation, leading to cell cycle arrest at G1, along with the downregulation of E2F1, CCNE1, MYBL2, and CDC25A expression. Overexpression of E2F1 restored the inhibited phenotype induced by SVIL-AS1 overexpression, suggesting that SVIL-AS1 suppresses LUAD cell proliferation by E2F1.

There are some limitations in this study. Firstly, we observed that SVIL-AS1 downregulation could

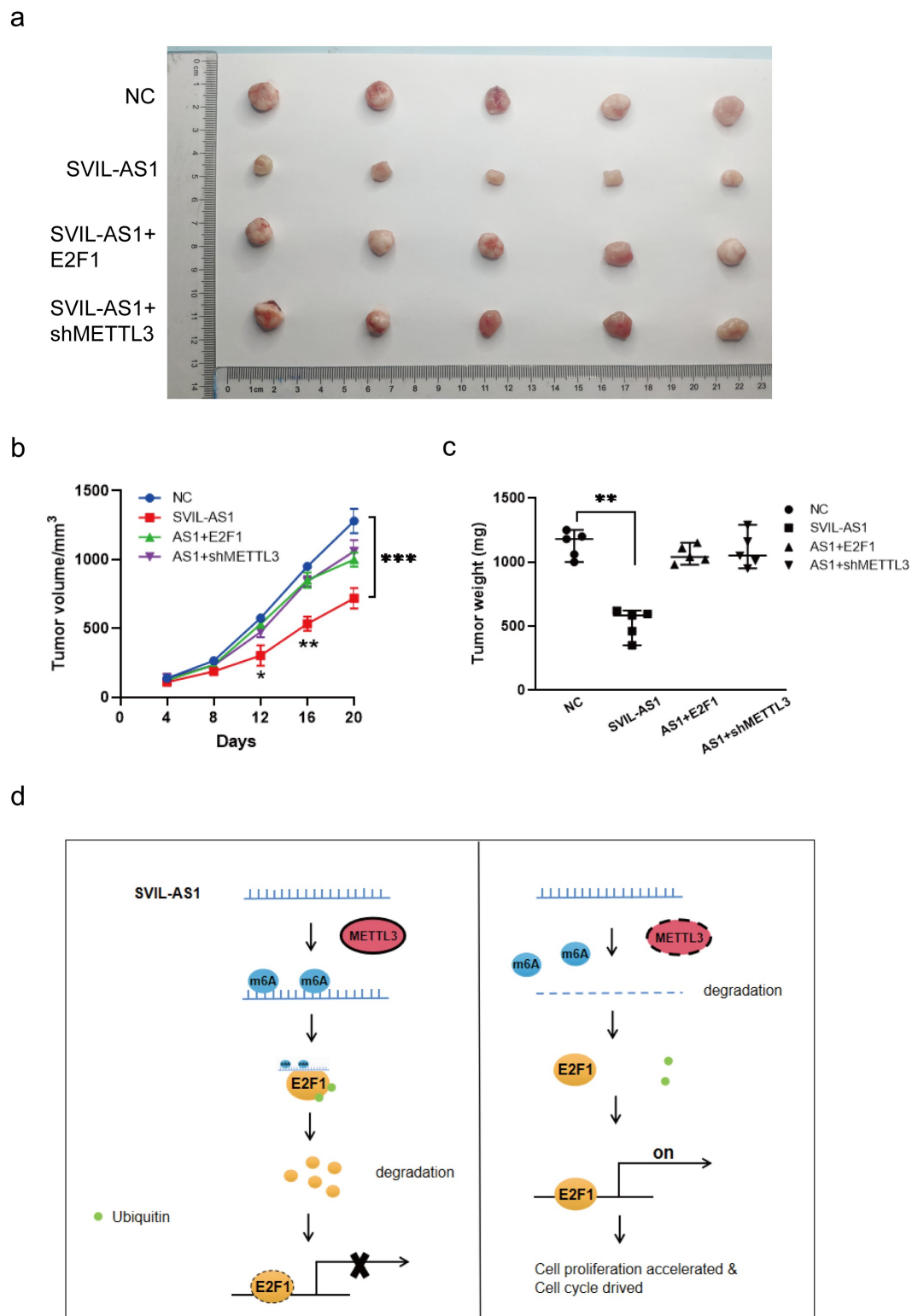


Figure 7. SVIL-AS1 reduced tumor growth *in vivo*. (a) A549 cells stably expressing SVIL-AS1, SVIL-AS1 plus E2F1 (SVIL-AS1 +E2F1), SVIL-AS1 plus METTL3 knockdown (SVIL-AS1+shMETTL3), and vector plus sh-NC (negative control, NC). Images of xenograft tumors in each group are shown (n = 5). (b) Tumor volumes were measured every 4 days, and growth curves were drawn. * p < 0.05, ** p < 0.01, *** p < 0.001. (c) Tumor weight was calculated for each group. ** p < 0.01. (d) Schematic illustration of the mechanism SVIL-AS1 regulated by METTL3 to suppress LUAD tumorigenesis by targeting E2F1 and its target genes.

enhance E2F1 protein level but have no effect on E2F1 transcription activity, considering SVIL-AS1 distributed in both nucleus and cytoplasm, we speculated that SVIL-AS1 might regulate E2F1 degradation at both RNA and protein level. The mechanism of SVIL-AS1 affecting RNA degradation is worth exploring. Second, it is worth exploring how lncRNA SVIL-AS1 accelerates the ubiquitin-proteasome degradation of E2F1. Third, we did not investigate the signaling pathways involved in METTL3-mediated SVIL-AS1.

Conclusions

In summary, our study verified the tumor-suppressive role of the lncRNA SVIL-AS1 in LUAD. SVIL-AS1 mediated and stabilized by the m6A methyltransferase METTL3 inhibits LUAD cell proliferation and induces cell cycle arrest via the METTL3/SVIL-AS1/E2F1 axis (Figure 7(d)), which inspires the understanding of m6A and lncRNA in lung cancer pathology and tumor biology. Moreover, m6A modified SVIL-AS1 might be used as a potential prognostic biomarker and clinical target for LUAD.

Disclosure statement

No potential conflict of interest was reported by the author(s).

Funding

The author(s) reported there is no funding associated with the work featured in this article.

Author contributions

Zedong HU, Liang ZHU, Yilin ZHANG, Bing CHEN

B.C. designed and supervised the project. Z.H. performed the majority of the experiments, analysed the data, and wrote the manuscript. L.Z. and Y.Z. performed bioinformatics analysis and cell culture experiments. All authors discussed the results and commented on the manuscript.

References

- [1] Serke M, Schönfeld N. Diagnosis and staging of lung cancer. *Dtsch Med Wochenschr.* 2007;132(21):1165–1169.
- [2] Spiro SG, Tanner NT, Silvestri GA, et al. Lung cancer: progress in diagnosis, staging and therapy. *Respirology.* 2010;15(1):44–50
- [3] Yang L, Parkin DM, Ferlay J, et al. Estimates of cancer incidence in China for 2000 and projections for 2005. *Cancer Epidemiol Biomarkers Prev.* 2005;14:243–250.
- [4] Guttman M, Amit I, Garber M, et al. Chromatin signature reveals over a thousand highly conserved large non-coding RNAs in mammals. *Nature.* 2009;458:223–227.
- [5] Moran VA, Perera RJ, Khalil AM. Emerging functional and mechanistic paradigms of mammalian long non-coding RNAs. *Nucleic Acids Res.* 2012;40:6391–6400.
- [6] Necseulea A, Soumillon M, Warnefors M, et al. The evolution of lncRNA repertoires and expression patterns in tetrapods. *Nature.* 2014;505:635–640.
- [7] Akdm R, Rajkumar T, Mani S. Perspectives of long non-coding RNAs in cancer. *Mol Biol Rep.* 2017;44:203–218.
- [8] Toden S, Zumwalt TJ, Goel A. Non-coding RNAs and potential therapeutic targeting in cancer. *Biochimica et biophysica acta. Rev Cancer.* 2021;1875:188491.
- [9] Chandra GS, Nandan TY. Potential of long non-coding RNAs in cancer patients: from biomarkers to therapeutic targets. *Int J Cancer.* 2017;140:1955–1967.
- [10] Chi Y, Wang D, Wang J, et al. Long non-coding RNA in the pathogenesis of cancers. *Cells.* 2019;8(9):1015.
- [11] Esteller M. Non-coding RNAs in human disease. *Nat Rev Genet.* 2011;12(12):861–874.
- [12] Acha-Sagredo A, Uko B, Pantazi P, et al. Long non-coding RNA dysregulation is a frequent event in non-small cell lung carcinoma pathogenesis. *Br J Cancer.* 2020;122(7):1050–1058.
- [13] Ma Z, Ji J. N6-methyladenosine (m6A)RNA modification in cancer stem cells. *Stem Cells.* 2020;38(12):1511–1519.
- [14] Widagdo J, Anggono V. The m6A-epitranscriptomic signature in neurobiology: from neurodevelopment to brain plasticity. *J Neurochem.* 2018;147(2):137–152.
- [15] Zhang H, Shi X, Huang T, et al. Dynamic landscape and evolution of m6A methylation in human. *Nucleic Acids Res.* 2020;48(11):6251–6264.
- [16] Huang H, Weng H, Chen J. m6A modification in coding and non-coding RNAs: roles and therapeutic implications in cancer. *Cancer Cell.* 2020;37:270–288.
- [17] Liu ZX, Li LM, Sun HL, et al. Link between m6A modification and cancers. *Front Bioeng Biotechnol.* 2018;6:89.
- [18] Liu P, Zhang B, Chen Z, et al. m6A-induced lncRNA MALAT1 aggravates renal fibrogenesis in obstructive nephropathy through the miR-145/FAK pathway. *Aging (Albany NY).* 2020;12(6):5280–5299.
- [19] Yang C, Fan Z, Yang J. m6A modification of lncRNA MALAT1: a novel therapeutic target for myocardial ischemia-reperfusion injury. *Int J Cardiol.* 2020;306:162.
- [20] Xue L, Li J, Lin Y, et al. m6A transferase METTL3-induced lncRNA ABHD11-AS1 promotes the Warburg effect of non-small-cell lung cancer. *J Cell Physiol.* 2021;236(4):2649–2658.
- [21] Allmann S, Mayer L, Olma J, et al. Benzo[a]pyrene represses DNA repair through altered E2F1/E2F4 function marking an early event in DNA damage-induced cellular senescence. *Nucleic Acids Res.* 2020;48(21):12085–12101.

- [22] Denechaud PD, Fajas L, Giral A. E2F1, a novel regulator of metabolism. *Front Endocrinol (Lausanne)*. 2017;8:311.
- [23] Ertosun MG, Hapil FZ, Osman Nidai O. E2F1 transcription factor and its impact on growth factor and cytokine signaling. *Cytokine Growth Factor Rev*. 2016;31:17–25.
- [24] Singh S, Yennamalli RM, Gupta M, et al. Identification of nsSNPs of transcription factor E2F1 predisposing individuals to lung cancer and head and neck cancer. *Mutat Res*. 2020;821:111704.
- [25] Dimitrov D, Konstantinov D. Choice of x-ray diagnostic methods in chronic odontogenic sinusitis. *Radiologia diagnostica*. 1989;30:67–71.
- [26] Fang Z, Lin M, Li C, et al. A comprehensive review of the roles of E2F1 in colon cancer. *Am J Cancer Res*. 2020;10:757–768.
- [27] Feng DD, Cao Q, Zhang DQ, et al. Transcription factor E2F1 positively regulates interferon regulatory factor 5 expression in non-small cell lung cancer. *Onco Targets Ther*. 2019;12:6907–6915.
- [28] Zheng X, Huang M, Xing L, et al. The circRNA circSEPT9 mediated by E2F1 and EIF4A3 facilitates the carcinogenesis and development of triple-negative breast cancer. *Mol Cancer*. 2020;19:73.
- [29] Zhi T, Jiang K, Xu X, et al. ECT2/PSMD14/PTTG1 axis promotes the proliferation of glioma through stabilizing E2F1. *Neuro Oncol*. 2019;21:462–473.
- [30] Gyórfy B, Surowiak P, Budczies J, et al. Online survival analysis software to assess the prognostic value of biomarkers using transcriptomic data in non-small-cell lung cancer. *PLoS One*. 2013;8(12):e82241.
- [31] Liu J, Lichtenberg T, Hoadley KA, et al. An integrated TCGA pan-cancer clinical data resource to drive high-quality survival outcome analytics. *Cell*. 2018;173(2):400–416.e11.
- [32] Tang Z, Kang B, Li C, et al. GEPIA2: an enhanced web server for large-scale expression profiling and interactive analysis. *Nucleic Acids Res*. 2019;47(W1):W556–W560.
- [33] Peng Z, Wang J, Shan B, et al. Genome-wide analyses of long noncoding RNA expression profiles in lung adenocarcinoma. *Sci Rep*. 2017;7(1):15331.
- [34] Livak KJ, Schmittgen TD. Analysis of relative gene expression data using real-time quantitative PCR and the 2^{(-Delta Delta C(T))} method. *Methods*. 2001;25(4):402–408.
- [35] Dominissini D, Moshitch-Moshkovitz S, Salmon-Divon M, et al. Transcriptome-wide mapping of N(6)-methyladenosine by m(6)A-seq based on immunocapturing and massively parallel sequencing. *Nat Protoc*. 2013;8(1):176–189.
- [36] Chen CY, Ezzeddine N, Shyu AB. Messenger RNA half-life measurements in mammalian cells. *Methods Enzymol*. 2008;448:335–357.
- [37] Zhou Y, Zeng P, Li YH, et al. SRAMP: prediction of mammalian N6-methyladenosine (m6A) sites based on sequence-derived features. *Nucleic Acids Res*. 2016;44(10):e91.
- [38] Jingushi K, Aoki M, Ueda K, et al. ALKBH4 promotes tumorigenesis with a poor prognosis in non-small-cell lung cancer. *Sci Rep*. 2021;11(1):8677.
- [39] Yang X, Feng M, Jiang X, et al. miR-449a and miR-449b are direct transcriptional targets of E2F1 and negatively regulate pRb-E2F1 activity through a feedback loop by targeting CDK6 and CDC25A. *Genes Dev*. 2009;23(20):2388–2393.
- [40] Park MT, Lee SJ. Cell cycle and cancer. *J Biochem Mol Biol*. 2003;36(1):60–65.
- [41] Wang F, Zhang L. p15(INK4b) regulates cell cycle signaling in hippocampal astrocytes of aged rats. *Aging Clin Exp Res*. 2016;28(5):813–821.
- [42] Velásquez ZD, López-Osorio S, Waiger D, et al. Eimeria bovis infections induce G(1) cell cycle arrest and a senescence-like phenotype in endothelial host cells. *Parasitology*. 2021;148(3):341–353.
- [43] Archer K, Broskova Z, Bayoumi AS, et al. Long non-coding RNAs as master regulators in cardiovascular diseases. *Int J Mol Sci*. 2015;16(10):23651–23667.
- [44] Ravnskjaer K. Keystone symposia on epigenomics and chromatin dynamics: keystone resort, CO, January 17–22, 2012. *Epigenetics*. 2012;7(5):522–523.
- [45] Chan JJ, Tay Y. Noncoding RNA:RNA regulatory networks in cancer. *Int J Mol Sci*. 2018;19(5):1310.
- [46] Fang Y, Fullwood MJ. Roles, functions, and mechanisms of long non-coding RNAs in cancer. *Genomics Proteomics Bioinformatics*. 2016;14:42–54.
- [47] Castro-Oropeza R, Melendez-Zajgla J, Maldonado V, et al. The emerging role of lncRNAs in the regulation of cancer stem cells. *Cell Oncol (Dordr)*. 2018;41:585–603.
- [48] Huarte M. The emerging role of lncRNAs in cancer. *Nat Med*. 2015;21:1253–1261.
- [49] Wang Y, Lu JH, Wu QN, et al. LncRNA LINRIS stabilizes IGF2BP2 and promotes the aerobic glycolysis in colorectal cancer. *Mol Cancer*. 2019;18:174.
- [50] Li H, Tong F, Meng R, et al. E2F1-mediated repression of WNT5A expression promotes brain metastasis dependent on the ERK1/2 pathway in EGFR-mutant non-small cell lung cancer. *Cell Mol Life Sci*. 2021;78(6):2877–2891.
- [51] Meng Q, Liu M, Cheng R. LINC00461/miR-4478/E2F1 feedback loop promotes non-small cell lung cancer cell proliferation and migration. *Biosci Rep*. 2020;40(2). DOI:10.1042/BSR20191345
- [52] Shi J, Li J, Yang S, et al. LncRNA SNHG3 is activated by E2F1 and promotes proliferation and migration of non-small-cell lung cancer cells through activating TGF- β pathway and IL-6/JAK2/STAT3 pathway. *J Cell Physiol*. 2020;235(3):2891–2900.
- [53] Li X, Yang S, Zhang M, et al. Downregulation of SRPK2 promotes cell cycle arrest though E2F1 in non-small cell lung cancer. *Eur J Histochem*. 2019;63(4). DOI:10.4081/ejh.2019.3067